EPIC-PN OBSERVATIONS OF CYGNUS X-1

J. Wilms[1], E. Kendziorra[2], M.A. Nowak[3], K. Pottschmidt[4], F.W. Haberl[5], M. Kirsch[6], and S. Fritz[2]

[1]Department of Physics, University of Warwick, Coventry, CV4 7AL, United Kingdom
[2]Institut für Astronomie und Astrophysik, Abt. Astronomie, Universität Tübingen, 72074 Tübingen, Germany
[3]MIT-CXC, NE80-6077, 77 Massachusetts Ave., Cambridge, MA 02139, USA
[4]Center for Astrophysics and Space Sciences, University of California at San Diego, La Jolla, CA 92093-0424, USA
[5]Max Planck Institut für extraterrestrische Physik, Giessenbachstr., 85748 Garching, Germany
[6]ESA/ESAC, PO Box 50727, 28080 Madrid, Spain

ABSTRACT

In 2004 October and November we observed the black hole candidate four times with *XMM-Newton*'s EPIC-pn camera and simultaneously with the Rossi X-ray Timing Explorer (*RXTE*) and *INTEGRAL*. We present preliminary results on the analysis of the X-ray spectrum and on the source variability, presenting the highest signal to noise ratio data of the Fe Kα region of the source ever obtained.

Key words: Black Hole Physics, Cygnus X-1.

1. INTRODUCTION: SCIENCE FROM BRIGHT SOURCES

While a large amount of *XMM-Newton*'s observing time is devoted to the study of faint objects at high z or of X-ray binaries in other galaxies, observations of bright, i.e., high countrate, X-ray sources are nevertheless crucial for our detailed understanding of the physics of many of these objects. It is only with very high signal to noise data from such sources that we can study the physics of accretion to the level needed for understanding the phenomenology of fainter sources.

Many of the questions currently asked in the study of Active Galactic Nuclei (AGN), for example, are very similar to those also asked in the framework of Galactic black hole binaries (BHBs), and often studying both types of systems results in complementary information. For both, AGN and BHBs, the structure of the accretion flow close to the central black hole is still unclear. Current models range from those that explain the broad band spectrum in terms of a patchy Comptonizing electron plasma (the "accretion disk corona") sandwiching a more or less thin accretion disk, perhaps with an inner hot region (e.g., Dove et al., 1997; Petrucci et al., 2001; Zdziarski et al., 2003; Coppi, 2004), to those suggesting that the X-rays are due to emission from hot spots sitting "above" the black hole (Henri & Petrucci, 1997; Martocchia et al., 2002). It has recently been suggested that these hot spots could be forming the base of the radio jets now observed in these systems, and that possibly the whole X-ray continuum is due to the jets (Markoff et al., 2003, 2005).

In this contribution, we concentrate on two observational tools that could shed more light on the accretion geometry:

1. High signal to noise observations of spectral signatures which depend on the physical processes at work close to the black hole are often sensitive to the accretion geometry. The most promising of these signatures are relativistically broadened Fe Kα lines (e.g., Reynolds & Nowak, 2003; Wilms et al., 2001; Fabian et al., 2000). The shape of the lines depends on the observer's viewing angle with respect to the accretion disk, the Fe Kα emissivity of the accretion disk, and the angular momentum of the black hole. The different accretion geometries discussed above therefore result in different line profiles (e.g., Dovčiak et al., 2004), which could be detected in data with a high enough signal to noise ratio.
2. Accreting black holes show variability on all time scales, with Galactic sources having strong (30% rms) short term variability out to >100 Hz in their hard state. The nature of the variability can again be used to constrain the geometry of the accretion flow (Churazov et al., 2001; Uttley et al., 2005, and therein). For example, in hard state BHBs a time lag between hard and soft X-rays is observed, which is on the order of $\gtrsim$0.01 s for light curves centred on $\sim$2 keV and $\sim$10 keV (Pottschmidt et al., 2000; Nowak et al., 1999b). This X-ray lag is strongly dependent on the source state, with lags in transitional states between the hard state and the (accretion disk dominated) soft state being significantly larger than what is seen in the hard and soft state (Pottschmidt et al., 2000, 2003;

Table 1. EPIC data modes (after Ehle et al. 2005).

	Time res.	Live time [%]	Max. cps	mCrab
MOS				
Full frame (600×600)	2.6 s	100.0	0.70	0.24
Large window (300×300)	900 ms	99.5	1.8	0.6
Small window (100×100)	300 ms	97.5	5	1.7
Timing uncompressed (100×600)	1.5 ms	100.0	100	35
pn				
Full frame (376×384)	73.4 ms	99.9	8	0.9
Ext. full frame (378×384)	200 ms	100.0	3	0.39
Large window (198×384)	48 ms	94.9	12	1.3
Small window (63×64)	6 ms	71.0	130	14
Timing (64×200)	30 μs	99.5	1500	160
Burst (64×180)	7 μs	3.0	60000	6300

Kalemci et al., 2003). The magnitude of the time lag and its frequency dependence are such that they can not be explained, e.g., by invoking the diffusion time scale due to Compton scattering in the accretion disk corona (Nowak et al., 1999b), but rather consistent with what one would expect for typical jet sizes (similar lags in AGN, however, seem to be consistent with Comptonization).

All of the (potential) diagnostics discussed above require very high signal to noise data of high time resolution, if possible combined with good energy resolution. These requirements imply observations of bright sources, with an instrument of sufficiently high effective area, and with at least Silicon energy resolution.

Due to the presence of a relativistic Fe Kα line (Miller et al., 2002), its strong and energy dependent X-ray variability (Nowak et al., 1999a,b), and its well understood long term variability from the *RXTE* monitoring performed by our group (Wilms et al., 2005), a prime candidate for such studies is the Galactic black hole Cygnus X-1. Using *XMM-Newton*, *RXTE* and *INTEGRAL*, in 2004 Oct/Nov we therefore performed a set of four 10–20 ksec long observations of Cyg X-1, making full use of the high signal to noise provided by the instrument above $\sim$3 keV. Until the end of 2004, Cyg X-1 was in *XMM-Newton*'s Earth avoidance zone, such that the observations presented here are amongst the first *XMM-Newton* observations of Cyg X-1. Here, we give first results of the *XMM-Newton* data, results from the other satellites are presented by Fritz et al. (these proceedings).

2. CYG X-1 WITH *XMM-NEWTON*: PRELIMINARY RESULTS

2.1. High Time Resolution Observations with *XMM-Newton*

The EPIC instruments on *XMM-Newton* fulfill the requirements discussed in the last section, and especially the EPIC-pn camera provides a variety of data modes with a time resolution of better than a 100 ms. As shown in Table 1, however, most of these data modes only allow observations of comparably weak sources. The only mode allowing observations of very bright sources is the EPIC-pn Burst mode. This mode, however, has a very low efficiency with a duty cycle of only 3% and shows strong aliasing at high frequencies (Kuster et al., 1999). While studying broad band variability is possible in the Burst Mode, it is not ideal and 97% of all photons are not detected. The most ideal mode providing a high time resolution is therefore the EPIC-pn Timing Mode. In this mode the CCD is read out continuously, resulting in a very high duty cycle. A drawback, however, is the comparably low maximum source brightness of only 160 mCrab, making sources such as Cyg X-1, with typically $\sim$300 mCrab, unobservable.

This threshold count rate is not due to a physical limitation of the detector, however, but is rather due to the telemetry limitation of the *XMM-Newton* spacecraft. By increasing the telemetry allotted to the EPIC-pn it is possible to increase the maximum count rate and thus to decrease the danger of the data handling unit of the instrument switching to counting mode, where the transmission of individual events from the EPIC-pn camera is stopped and only the number of events dropped is transmitted. Since all data modes of the EPIC-MOS cameras are limited to sources with $<$35 mCrab, such an increase can be obtained by switching off the MOS without the loss of useful scientific information of the source under study. Despite the increase in available telemetry bandwidth for the EPIC-pn to somewhat over 1000 cps, this approach is not sufficient to allow studies of sources with a few 100 mCrab.

For our *XMM-Newton* observations of Cyg X-1, we therefore suggested using a modified version of the EPIC-pn Timing Mode. As outlined in further detail by Kendziorra et al. (2004), in addition to switching off the EPIC-MOS, we increase the EPIC-pn lower energy threshold for events to be transmitted. Since for many studies of black holes the most interesting information for spectral-temporal studies is found in the $>$3 keV band, we increase the lower energy threshold of the Timing Mode from its standard value of 200 eV to 2.8 keV. In this band (and depending on the source state) Cyg X-1

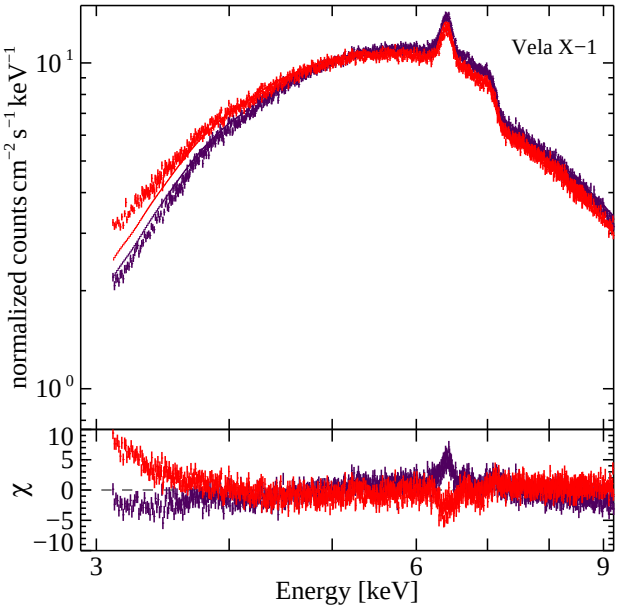

Figure 1. Comparison of a standard EPIC-pn Timing Mode observation of Vela X-1 (dark) with a simulated Modified Timing Mode observation (red/lighter gray), showing the redistribution of events towards lower energies due to the increased lower energy threshold of the Modified Timing Mode.

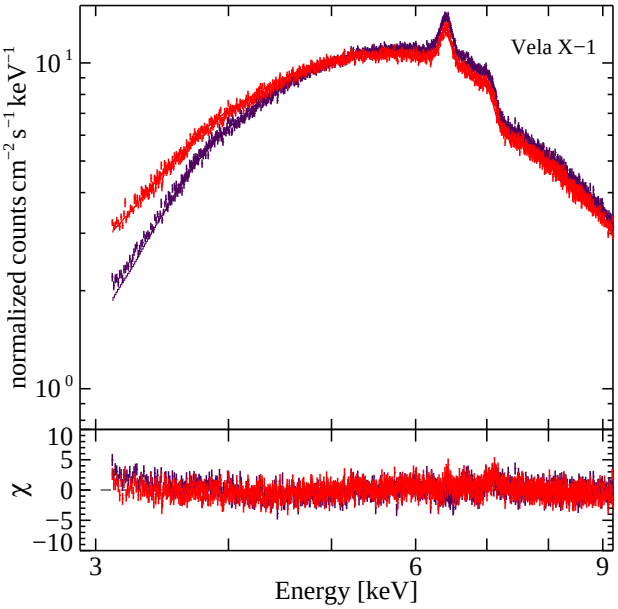

Figure 2. Same data as in Fig. 1, but using a special response matrix for the Modified Timing Mode. The new response matrix accounts for the different sensitivity and the spectral softening introduced by the Modified Timing Mode.

delivers 500–800 cps. This means that all data measured above the threshold can be transmitted to Earth and that high time resolution, low deadtime measurements can be made in the iron band with Silicon resolution.

2.2. Calibrating the Modified Timing Mode

A problem of increasing the lower energy threshold of the EPIC-pn camera is that a recalibration of the instrument is required. This need arises from the fact that no combination of split events is performed on-board the satellite. Rather, information about the charge deposited by the incoming X-rays in each pixel is transmitted to ground separately and then combined during the first step of the EPIC-pn data analysis. As the lower energy threshold of the EPIC-pn is increased, a larger fraction of the split partners is not transmitted to Earth. Loosing these split partners means that the energy reconstruction for double and higher grade events cannot be performed. As a result, the energy resolution of the Modified Timing Mode is slightly reduced and the redistribution of events is changed. Figure 1 shows this effect by comparing the spectrum of Vela X-1 as taken with the standard Timing Mode with a simulated Modified Timing Mode observation, which was obtained by filtering the raw Vela X-1 event data before event recombination and discarding all events with energies below 2.8 keV. Due to the lack of a significant fraction of split partners in the Modified Timing Mode, spectra taken in that mode appear softer since double (and higher grade) events missing their split partners now show up as single events with a correspondingly lower energy.

Using the available Timing Mode observations from the *XMM-Newton* archive it is possible to build a new detector response matrix that takes these effects into account. Figure 2 shows the result of fitting the simulated and measured data of Vela X-1 using this new detector response matrix. The matrix accounts for most features introduced by the Modified Timing Mode and the residuals of the Modified and the standard Timing Mode are very similar. Note that no attempt is made in this demonstration to obtain a good fit to the data, e.g., the clear residuals present in the Fe K edge region. The quality of the response matrix is demonstrated, however, by considering that both residuals are very similar (i.e., equally bad).

We conclude that the overall calibration of the Modified Timing Mode is satisfactory, however, there are still some questions remaining. For example, the high count rate in the EPIC-pn leads to an improvement of the charge transfer efficiency (CTE) of the detector compared to dimmer sources, which is not yet taken into account. The absolute energy calibration of the data presented in the following is therefore not yet up to the level of the EPIC-pn standard data modes and all energy values given below could be slightly too high since the standard data reduction pipelines assume a lower CTE and consequently overcompensate during the derivation of pulse height invariant energy values in the case of bright source observations. Furthermore, not all measurements entering the build process of the new response matrix have been completely checked. Due to these reasons, in the following

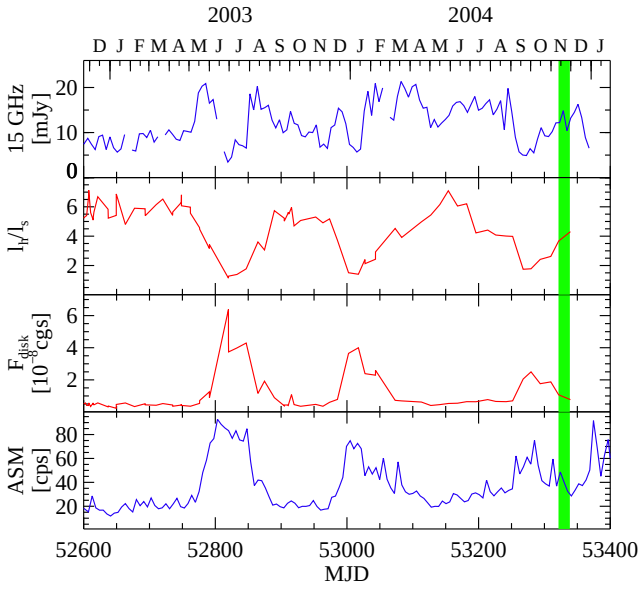

Figure 3. Results from RXTE and Ryle radio telescope monitoring of Cyg X-1 in 2003 and 2004, based on Comptonization fits. Shown from top to bottom are the 15 GHz radio flux, the ratio l_h/l_s of the compactness of the accretion disk corona, l_h, and of the accretion disk, l_s, which is a measure for the spectral hardness, the bolometric accretion disk flux, F_{disk}, and the RXTE-ASM count rate. The time interval of the XMM-Newton observations is shown by the vertical bar.

presentation of first scientific results from Cyg X-1 we will only give very few "hard numbers" and we will refrain from comparing our measurements with the simultaneous *RXTE* and *INTEGRAL* data.

2.3. Cyg X-1: Scientific Results

During our four *XMM-Newton*/*RXTE*/*INTEGRAL* observations, Cyg X-1 was in one of its transitional states between the hard state and the thermally dominated soft state (Fritz, these proceedings). Figure 3 shows the history of the source in the context of the *RXTE* and radio monitoring campaign performed by our group (Wilms et al., 2005; Pottschmidt et al., 2003). This state is very interesting for a further scientific study, since *RXTE* and *Chandra* observations have shown it to be characterized by radio flaring and complex X-ray timing behavior, as well as the presence of a relativistically broadened Fe Kα line.

The increased soft X-ray emission during the intermediate state, however, leads to an increased pile-up in the center of the point spread function compared to a pure hard state. In the following analysis we therefore ignored data from the centermost 3 CCD columns. For the case of observation 2 (20/21 Nov. 2004), this means that we ignore 7000000 of the 17000000 events detected above 2.8 keV in this $\sim$17 ksec long observation.

As shown in Fig. 4 the signal to noise ratio of the remaining data is still sufficient for spectral analysis. Since the raw data clearly show the presence of a narrow line around 6.4 keV, we first model the spectrum outside the 5–8 keV iron band with a power law. Using this continuum, we find that clear residuals remain in the Fe Kα region, which can be described by a narrow feature at $\sim$6.5 keV plus a further broad feature (Fig. 4). Due to this reason, a power law fit to the whole 4–9 keV spectrum does not result in an acceptable χ^2.

Modelling the data now with a power law and iron features shows that both, a narrow ($\sigma = 80 \pm 35$ eV) Fe line at 6.52 ± 0.02 keV with equivalent width of 14 eV and a relativistic Kerr line from ionized iron ($E = 6.7 \pm 0.1$ keV) with an emissivity $\propto r^{-4.3\pm0.1}$ and an equivalent width of 400 eV are required for a satisfactory description of the data ($\chi^2_{\rm red} = 1.3$). These parameters are similar to earlier *Chandra* intermediate state observations of a relativistic line in Cyg X-1 (Miller et al., 2002). Differences in the line parameters can be attributed to the dynamic nature of the accretion disk geometry, which is generally taken to be in the process of reconfiguring during the intermediate state. Our *XMM-Newton* observations thus provide independent confirmation for the presence of a relativistic line during the intermediate state.

We stress again, however, that these results are based on a not yet finalized calibration of the Modified Timing Mode. For example, the energy of the line features could be slightly lower than quoted above, due to the overcompensation caused by the improved CTE in bright source. In addition, similarly good fits can also be obtained by adding a strong Fe K-edge, as could be due to strong Compton reflection, to the data, without requiring the presence of a strong and broad line. This result is reminiscent of current discussions about the interpretation of similar strong features in narrow line Seyfert 1 galaxies, which can equally well be described either by reflection dominated spectra or strong relativistic Fe Kα lines (Boller et al., 2003; Pounds et al., 2003; Fabian et al., 2004). For the case of Cyg X-1, a final verdict on the nature of the iron features will therefore only be available once the simultaneous *RXTE* and *INTEGRAL* data are added to our spectral analysis.

We finally turn to X-ray time lags as an example for the X-ray timing capabilities of *XMM-Newton*. The left hand side of Fig. 5 shows the X-ray time lag measured in two narrow bands. The X-ray lag is reminiscent of lags determined previously in the intermediate state with *RXTE* in similar bands (Fig. 5, right, see also Pottschmidt et al. 2000), independently confirming the classification of the source state from the spectral data. Compared to proportional counters such as the *RXTE*-PCA, however, the energy resolution possible with Si-based detectors such as the EPIC-pn is much higher. For example, in a preliminary analysis of the energy dependent root-mean-square variability of our data, we find a clear drop in rms in the Fe Kα band, akin to similar behavior seen at lower resolution in BHBs and AGN (Markowitz et al., 2003; Życki, 2004, and therein).

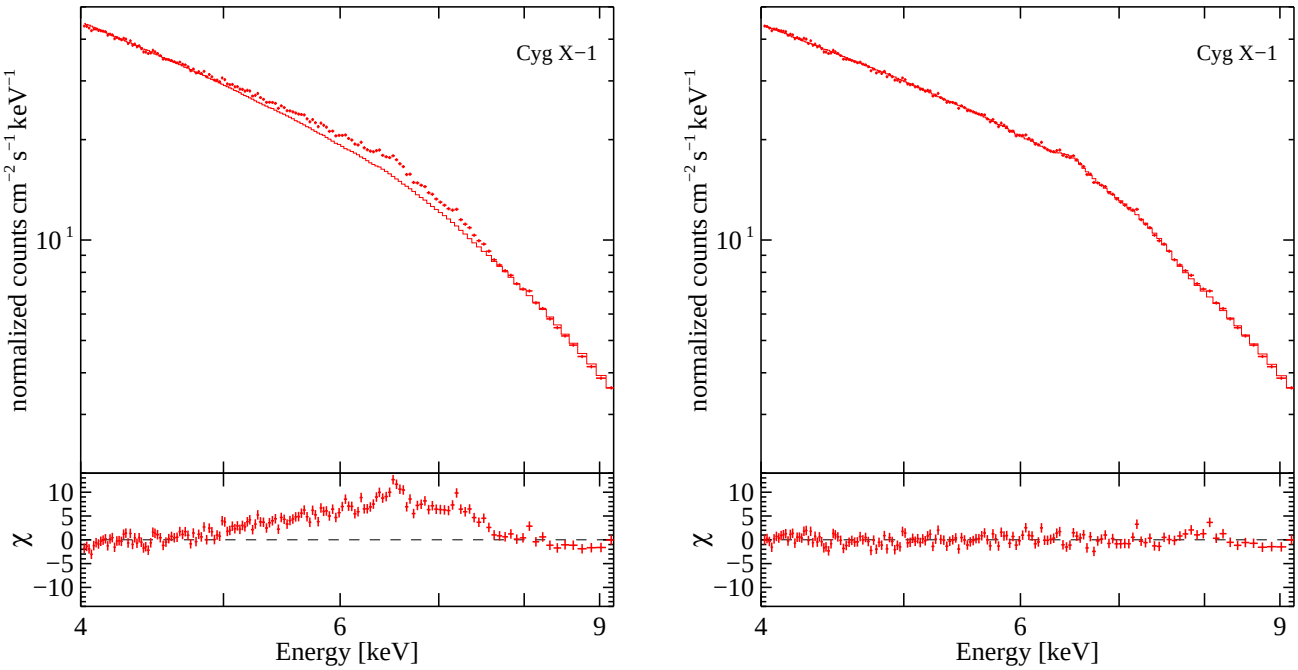

Figure 4. Left: A power-law fit to the EPIC-pn data from obs. 2 measured outside of the 5–8 keV band reveals strong residuals in the Fe Kα region, possibly pointing towards the presence of a relativistic line. Right: Same data, but fitting the whole band with a power law and a narrow and a relativistic line.

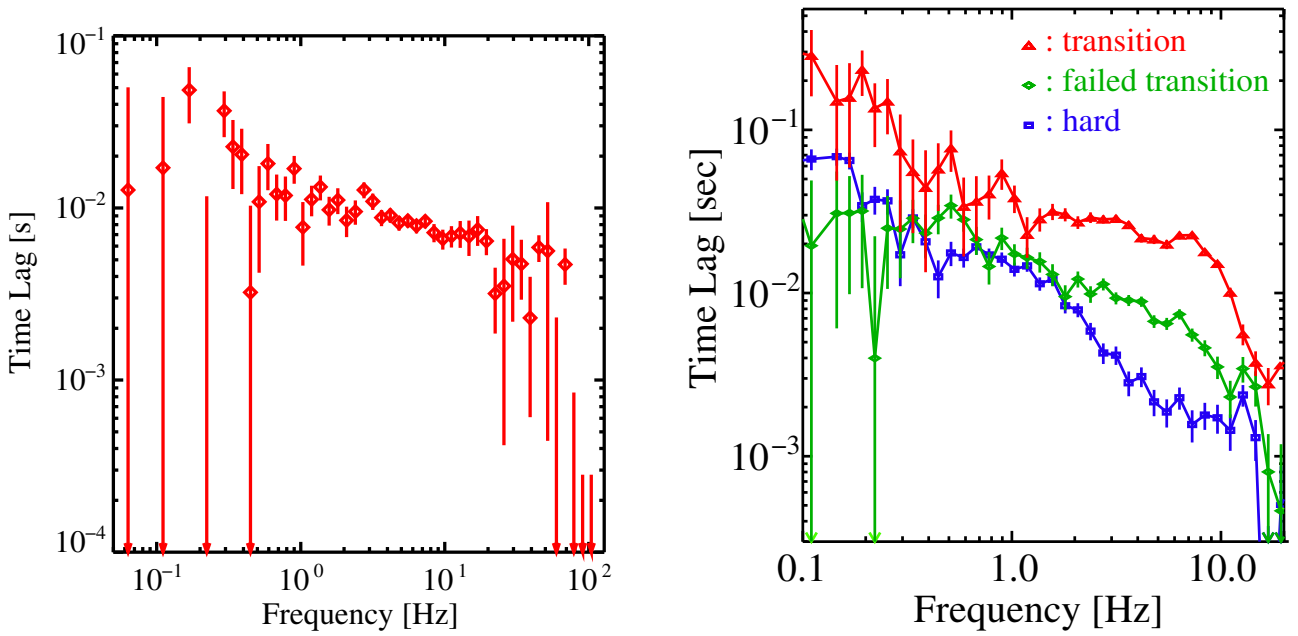

Figure 5. Left: Fourier frequency dependency of the 3.5–5.5 keV vs. 6.0–8.5 keV X-ray time lags obtained for XMM-Newton obs. 2. A positive lag means that the hard X-rays lag the soft ones. Right: 2.5–4 keV vs. 8–13 keV X-ray time lags determined with RXTE for different spectral states of Cyg X-1 (Pottschmidt et al., 2000).

3. SUMMARY AND OUTLOOK

The results presented in the previous sections indicate the significant scientific potential of *XMM-Newton* for studies of the Fe Kα band from in bright Galactic sources with the Modified Timing Mode of the EPIC-pn camera. These results include the possible confirmation of the presence of a relativistic Fe Kα line during the intermediate state of Cyg X-1. We are optimistic that the remaining issues related to the final calibration of the mode and understanding the pile-up issues, will be solved within the next few months after the submission of this contribution. The final results from the calibration will be made available to the community in the near future.

ACKNOWLEDGMENTS

The observations presented herein were made on behalf of a larger collaboration, which in addition to the authors consists of C. Brocksopp (UCL), P. Coppi (Yale), R.P. Fender (Southampton), M. van der Klis (Univ. Amsterdam), T. Maccarone (Southampton), G.G. Pooley (Univ. Cambridge), N.S. Schulz (MIT), and A.A. Zdziarski (Warsaw). This work is based on observations obtained with *XMM-Newton*, an ESA science mission with instruments and contributions directly funded by ESA member states and NASA. We thank all people who made the observations with the Modified Timing Mode possible. This work has been financed in part by DLR grant 50OR0302.

REFERENCES

Boller, T., Tanaka, Y., Fabian, A., et al. 2003, MNRAS, 343, L89

Churazov, E., Gilfanov, M., & Revnivtsev, M. 2001, MNRAS, 321, 759

Coppi, P. 2004, in X-Ray Timing 2003: Rossi and Beyond, ed. P. Kaaret, F. K. Lamb, & J. Swank, Am. Inst. Phys., Conf. Ser. 714 (Woodbury: AIP), 79–88

Dove, J. B., Wilms, J., & Begelman, M. C. 1997, ApJ, 487, 747

Dovčiak, M., Karas, V., & Yaqoob, T. 2004, ApJS, 153, 205

Ehle, M., Breitfellner, M., González Riestra, R., et al. 2005, *XMM-Newton* Users' Handbook, available online at `http://xmm.vilspa.esa.es/external/xmm_user_support/documentation/uhb/index.html`

Fabian, A. C., Iwasawa, K., Reynolds, C. S., & Young, A. J. 2000, PASP, 112, 1145

Fabian, A. C., Miniutti, G., Gallo, L., et al. 2004, MNRAS, 353, 1071

Henri, G. & Petrucci, P. O. 1997, A&A, 326, 87

Kalemci, E., Tomsick, J. A., Rothschild, R. E., et al. 2003, ApJ, 586, 419

Kendziorra, E., Wilms, J., Haberl, F., et al. 2004, in Proc. SPIE 5488, 613–622

Kuster, M., Benlloch, S., Kendziorra, E., & Briel, U. G. 1999, in EUV, X-ray and Gamma-Ray Instrumentation for Astronomy X, eds. O. H. Siegmund & K. A. Flanagan, Proc. SPIE 3765 (Bellingham, WA: SPIE), 673–682

Markoff, S., Nowak, M., Corbel, S., Fender, R., & Falcke, H. 2003, A&A, 397, 645

Markoff, S., Nowak, M. A., & Wilms, J. 2005, ApJ, in press (astro-ph/0509028)

Markowitz, A., Edelson, R., & Vaughan, S. 2003, ApJ, 598, 935

Martocchia, A., Matt, G., & Karas, V. 2002, A&A, 383, L23

Miller, J. M., Fabian, A. C., Wijnands, R., et al. 2002, ApJ, 578, 348

Nowak, M. A., Vaughan, B. A., Wilms, J., Dove, J. B., & Begelman, M. C. 1999a, ApJ, 510, 874

Nowak, M. A., Wilms, J., Vaughan, B. A., Dove, J. B., & Begelman, M. C. 1999b, ApJ, 515, 726

Petrucci, P. O., Haardt, F., Maraschi, L., et al. 2001, ApJ, 556, 716

Pottschmidt, K., Wilms, J., Nowak, M. A., et al. 2000, A&A, 357, L17

Pottschmidt, K., Wilms, J., Nowak, M. A., et al. 2003, A&A, 407, 1039

Pounds, K. A., Reeves, J. N., Page, K. L., et al. 2003, MNRAS, 341, 953

Reynolds, C. S. & Nowak, M. A. 2003, Phys. Rep., 377, 389

Uttley, P., McHardy, I. M., & Vaughan, S. 2005, MNRAS, 359, 345

Wilms, J., Nowak, M. A., Pottschmidt, K., et al. 2005, A&A, in press (astro-ph/0510193)

Wilms, J., Reynolds, C. S., Begelman, M. C., et al. 2001, MNRAS, 328, L27

Zdziarski, A. A., Lubiński, P., Gilfanov, M., & Revnivtsev, M. 2003, MNRAS, 342, 355

Życki, P. T. 2004, MNRAS, 351, 1180